Proc. Natl. Acad. Sci. USA
Vol. 94, pp. 12431–12436, November 1997
Cell Biology

MAD2 associates with the cyclosome/anaphase-promoting complex and inhibits its activity

(mitotic checkpoint/spindle assembly checkpoint/cell cycle/mitosis)

YONG LI*†, CARLOS GORBEA†‡, DAVID MAHAFFEY‡, MARTIN RECHSTEINER‡, AND ROBERT BENEZRA*§

*Cell Biology Program, Memorial–Sloan Kettering Cancer Center, 1275 York Avenue, New York, NY 10021; and ‡Department of Biochemistry, University of Utah School of Medicine, Salt Lake City, UT 84132

Communicated by Mario R. Capecchi, University of Utah School of Medicine, Salt Lake City, UT, September 11, 1997 (received for review July 23, 1997)

ABSTRACT **Cell cycle progression is monitored by checkpoint mechanisms that ensure faithful duplication and accurate segregation of the genome. Defects in spindle assembly or spindle-kinetochore attachment activate the mitotic checkpoint. Once activated, this checkpoint arrests cells prior to the metaphase-anaphase transition with unsegregated chromosomes, stable cyclin B, and elevated M phase promoting factor activity. However, the mechanisms underlying this process remain obscure. Here we report that upon activation of the mitotic checkpoint, MAD2, an essential component of the mitotic checkpoint, associates with the cyclin B-ubiquitin ligase, known as the cyclosome or anaphase-promoting complex. Moreover, purified MAD2 causes a metaphase arrest in cycling *Xenopus laevis* egg extracts and prevents cyclin B proteolysis by blocking its ubiquitination, indicating that MAD2 functions as an inhibitor of the cyclosome. Thus, MAD2 links the mitotic checkpoint pathway to the cyclin B destruction machinery which is critical in controlling the metaphase-anaphase transition.**

Regulated proteolysis of a group of key cell cycle molecules, such as $p40^{SIC1}$ and cyclin B, plays a critical role in cell cycle progression (1, 2). These target proteins must first be ubiquitinated by the sequential action of three enzymes: E1 [ubiquitin (Ub)-activating enzyme], E2 (Ub-conjugating enzyme), and E3 (Ub ligase) (3). Once ubiquitinated, the target proteins are rapidly degraded by the 26S proteasome (4). The Ub-proteasome-mediated degradation of cyclin B is required for the exit from mitosis and persists until the onset of the next S phase (5–7). The cyclin B-Ub ligase, also termed the cyclosome or anaphase-promoting complex (APC), has recently been isolated and shown to be required for cyclin B ubiquitination *in vitro* (8–10). The cyclosome is a large protein complex with a sedimentation coefficient of 20 S in *Xenopus* eggs and clam oocytes and 36 S in budding yeast (8, 9, 11, 12). It becomes phosphorylated in M phase and phosphatase treatment inactivates the mitotic form of the cyclosome *in vitro* (9, 12, 13). The cyclosome/APC is composed of at least eight subunits including the *BIME, CDC16, CDC23*, and *CDC27* gene products, which are required for the metaphase-anaphase transition (4, 9, 11, 12, 14–16), providing further evidence that the cyclosome is involved in the degradation of the inhibitor(s) of this transition as well as cyclin B (17).

The metaphase-anaphase transition is monitored by the mitotic checkpoint, which senses spindle aberrations and responds by arresting the cell cycle, thereby preventing aberrant chromosome segregation (18–20). *MAD1*, *MAD2*, *MAD3*, *BUB1*, *BUB2*, *BUB3*, and *MPS1* have been identified as components of the mitotic checkpoint in budding yeast (18–20). Recently, *Xenopus* and human *MAD2* were isolated and shown to be required for the execution of the mitotic checkpoint in vertebrates (21, 22). Once activated, the mitotic checkpoint arrests the cell cycle prior to the metaphase-anaphase transition with unsegregated chromosomes and high levels of cyclin B, suggesting that the cyclosome might be the target of the response pathway.

In this report we show that: (*i*) MAD2 associates with the cyclosome/APC *in vivo* when the mitotic checkpoint is activated and dissociates upon checkpoint release; (*ii*) addition of exogenous MAD2 to cycling *Xenopus* egg extracts results in inhibition of cyclin B proteolysis and metaphase arrest; and (*iii*) MAD2 generates these effects by inhibiting the Ub ligase activity of the cyclosome.

MATERIALS AND METHODS

Cell Culture and Synchronization. HeLa cells were cultured in DMEM/high glucose supplemented with antibiotics and fetal bovine serum (10%). HeLa cells were synchronized in G_1/S with either 300 μM mimosine or 2 mM hydroxyurea for 12 hr, or in G_2/M with 100 nM nocodazole (NOC) for 24 hr. To arrest cells in mitosis, HeLa cells were treated with 50 nM NOC for 16 hr. Cells were then washed with PBS three times and subjected to mechanical shake-off. These cells were subsequently released into NOC-free medium for up to 6 hr.

Immunoprecipitations. HeLa cell extracts were prepared as described (22) and immunoprecipitated with affinity-purified anti-MAD2 or anti-CDC27. MAD2 (0.5 mg/ml) was added to Δ90-arrested *Xenopus* egg extract and incubated for 10 min at 23°C prior to immunoprecipitation with anti-CDC27 antibodies. The immunoprecipitates were washed six times with wash buffer (50 mM Tris·HCl, pH 7.5/250 mM NaCl/1% Nonidet P-40/0.1% SDS/2 mM EDTA/50 mM NaF/0.25 mM Na_3VO_4/1 mM phenylmethylsulfonyl fluoride/0.5 μg/ml aprotinin, antipain, pepstatin A, and leupeptin), and then resolved by SDS/PAGE and subjected to Western blot analysis as described (22).

Glycerol Gradient Sedimentation. HeLa extracts (1.5 mg) were layered atop 24–40% glycerol gradients and centrifuged at 25,000 rpm for 45.5 hr in a Beckman SW40 rotor. Fractions (0.9 ml) were collected from the bottom of the tube and 75 μl of each fraction was subjected to Western blot analysis as indicated.

Cell Cycle Progression in *Xenopus* Egg Extracts. Electrically activated *Xenopus* egg extract was prepared as described (23, 24). *Xenopus* sperm nuclei were prepared (23) and added to

The publication costs of this article were defrayed in part by page charge payment. This article must therefore be hereby marked "*advertisement*" in accordance with 18 U.S.C. §1734 solely to indicate this fact.

Abbreviations: APC, anaphase-promoting complex; Ub, ubiquitin; NOC, nocodazole.

†Y.L. and C.G. contributed equally to this paper.

§To whom reprint requests should be addressed. e-mail: r-benezra@ski.mskcc.org.

extract to a final concentration of 100 nuclei per μl. Newly synthesized proteins were labeled with [^{35}S]methionine added to a final concentration of 0.5 μCi/μl (1 Ci = 37 GBq). Purified human MAD2 protein (22) [or an equal volume of buffer (10 mM Tris·HCl, pH 7.4/10 mM NaCl) as a dilution control] was added to a final concentration of 50 μg/ml. Extract was incubated at 23°C to initiate cycling. Samples were taken at the indicated times. For [^{35}S]cyclin B proteolysis, 2 μl of extract was separated by SDS/PAGE (12.5% gel). Histone H1 kinase samples were diluted 1:50 and processed as described (23, 24). For the nuclear morphology assay, 1 μl of extract was treated with fixative (10% formaldehyde) containing Hoechst 33342 as described (23).

Mitotic *Xenopus* Egg Extracts. Interphase extract was prepared (23, 24) and cycloheximide was added to a final concentration of 0.1 mg/ml. Δ90-arrested extract was prepared as described (25, 26) by adding cyclin Δ90 to interphase extract and incubating for 40 min at 23°C. Cyclin degradation assays were initiated by adding [^{35}S]cyclin B2 to the reaction mixtures (2.2 μl per 20 μl extract). [^{35}S]cyclin was prepared as described (26) by *in vitro* translation in interphase *Xenopus* egg extract. Aliquots (3 μl) were withdrawn at the time indicated and analyzed by SDS/PAGE followed by PhosphorImager analysis (Molecular Dynamics) and autoradiography.

Degradation of Ub-^{125}I-Lysozyme Conjugates. Ub-^{125}I-lysozyme conjugates were prepared as described (27). Δ90-arrested extract (36 μl) was incubated with either buffer (10 mM Tris·HCl, pH 7.4/10 mM NaCl), MAD2 (1 mg/ml), or S5a (1 mg/ml) for 10 min at 23°C prior to the addition of Ub-^{125}I-lysozyme conjugates (12,700 cpm) in a final volume of 100 μl. Aliquots (25 μl) were taken at the time indicated, added to 0.875 ml of 1% BSA, and proteins were precipitated on ice with 100 μl of 100% trichloroacetic acid. The amount of trichloroacetic acid-soluble protein fragments in the supernatant fractions was counted in a Beckman Gamma 4000 counter for 10 min. The amount of trichloroacetic acid-soluble radioactivity in untreated conjugates was subtracted from the values shown.

Isopeptidase Activity Assay. Isopeptidase rates were measured as described previously (24). Briefly, Δ90-arrested extract was incubated either with buffer or MAD2 (0.5 mg/ml) for 10 min at 23°C. The reactions were started by adding the indicated volume of extract to 20 μl of Ub-^{125}I-lysozyme conjugates (9,200 cpm) and 0.5 μl of ATP-regenerating system. At the indicated times, each reaction was quenched with SDS sample buffer, subjected to SDS/PAGE, and the ^{125}I-lysozyme regenerated from Ub conjugates was quantitated by PhosphorImager analysis and calculated as a percentage of the total ^{125}I for each lane. The percentage of unconjugated ^{125}I-lysozyme present in untreated conjugates was subtracted from the values shown.

Ub-Conjugation Assay. Ub-conjugation rates were measured as described (24). Briefly, the reactions were initiated by adding 1 μl (3.9×10^5 cpm) of ^{125}I-Ub (70 μg/ml) to 30 μl of Δ90-arrested extract containing buffer or MAD2 (0.5 mg/ml). At the indicated times, 2 μl of extract was removed and quenched in SDS sample buffer. SDS/12.5% polyacrylamide gel was loaded with 24,000 cpm per lane and the percentage of radioactivity above 100 kDa (high molecular weight conjugates) was determined by PhosphorImager analysis. A slight increase in the amount of ^{125}I-Ub conjugates was produced in the presence of MAD2 relative to the control.

RESULTS AND DISCUSSION

It was first determined whether MAD2 is physically associated with the cyclosome in HeLa cells upon activation of the mitotic checkpoint by NOC treatment (22). As a control, HeLa cells were also arrested in G_1/S with mimosine or hydroxyurea (Fig. 1*A*). A decrease in the electrophoretic mobility of a portion of CDC27 was observed in NOC-arrested G_2/M extracts relative to G_1/S extracts (Fig. 1*B*). Since about half of the G_2/M population was actually arrested in M phase based on the measurement of the mitotic index (data not shown), our findings are consistent with significant phosphorylation of cyclosome components in mitosis (9, 12, 13). In G_1/S, MAD2 was associated with a small fraction of CDC27 (Fig. 1*B Left*; longer exposure also revealed low levels of CDC16 in the anti-MAD2 immunoprecipitates). However, when HeLa cells were arrested in G_2/M, a much higher proportion of CDC16/27 was immunoprecipitated by the anti-MAD2 antibody (Fig. 1*B Right*). In addition, anti-CDC27 immunoprecipitated both CDC16 and MAD2 from the G_2/M extracts, but not the G_1/S extracts, further confirming the MAD2-cyclosome association in G_2/M (Fig. 1*B Right*). Interestingly, we observed that MAD2 preferentially associated with the phosphorylated forms of CDC27 and CDC16 (Fig. 1*C*, compare lanes 3 and 6). Physical association between MAD2 and the phosphorylated cyclosome in G_2/M-arrested cells raises the possibility that MAD2 executes the mitotic checkpoint by direct association with the cyclosome.

To confirm that MAD2 was associated with the cyclosome, G_2/M and G_1/S HeLa cell extracts were subjected to glycerol gradient sedimentation. A fraction of MAD2 cosedimented with the phosphorylated cyclosome in G_2/M, but not with the cyclosome in G_1/S (Fig. 1*D*). Interestingly, unphosphorylated cyclosome in G_1/S extracts sedimented faster than the phosphorylated complex in G_2/M (Fig. 1*D*). These results document the association between MAD2 and the cyclosome and demonstrate that this interaction takes place preferentially when the mitotic checkpoint is activated.

The MAD2-cyclosome interaction was then monitored following the inactivation of the mitotic checkpoint. HeLa cells arrested in mitosis by NOC treatment were collected by shake-off and then replated into NOC-free medium. Cyclin B levels decreased significantly after release (Fig. 1*E*), indicating that a substantial portion of the HeLa cells had progressed through the mitotic arrest. Western blot analysis showed that MAD2 and CDC27 levels remained relatively unchanged as cells progressed through mitosis (Fig. 1*F Right*), yet anti-MAD2 antibodies immunoprecipitated significantly less CDC27 following removal of NOC (Fig. 1*F Left*). These data demonstrate that MAD2 dissociates from the cyclosome when the mitotic checkpoint becomes inactivated and suggests that dissociation may be necessary for the completion of mitosis.

The observed MAD2-cyclosome interactions suggest that MAD2 functions as an inhibitor of the cyclosome. To investigate the effect of MAD2 on cell cycle progression in an *in vitro* system, recombinant human MAD2 was added to cycling *Xenopus* egg extracts, and cell cycle progression was monitored by three criteria: cyclin B proteolysis, histone H1 kinase activity, and nuclear morphology (23) (Fig. 2). In the absence of exogenous MAD2, cyclin B was degraded between 60–70 min concomitant with a peak of histone H1 kinase activity, indicating that the extract had passed through mitosis (Fig. 2 *A* and *B*). Nuclear morphology also revealed that the extract had progressed through mitosis since by 60 min nuclear envelope breakdown occurred and condensed chromatin was associated with mitotic spindles (Fig. 2*C Left*), whereas by 100 min chromatin decondensed and interphase nuclei reformed. In sharp contrast, addition of MAD2 caused a metaphase arrest: cyclin B degradation was inhibited (Fig. 2*A*), histone H1 kinase activity rose to mitotic levels and remained elevated (Fig. 2*B*), mitotic spindles persisted, and chromatin remained highly condensed and aligned on spindles (Fig. 2*C Right*).

Mitotic *Xenopus* extracts were also used to determine whether MAD2 caused cyclin B stabilization by inhibiting the cyclin degradation pathway. A nondegradable form of cyclin B lacking the 90 N-terminal amino acids (cyclin Δ90) (25, 26) and the recombinant MAD2 were added simultaneously to inter-

A

Treatment	G1/S	G2/M
Mimosine	97%	3%
Hydroxyurea	98%	2%
Nocodazole	16%	84%
None	84%	16%

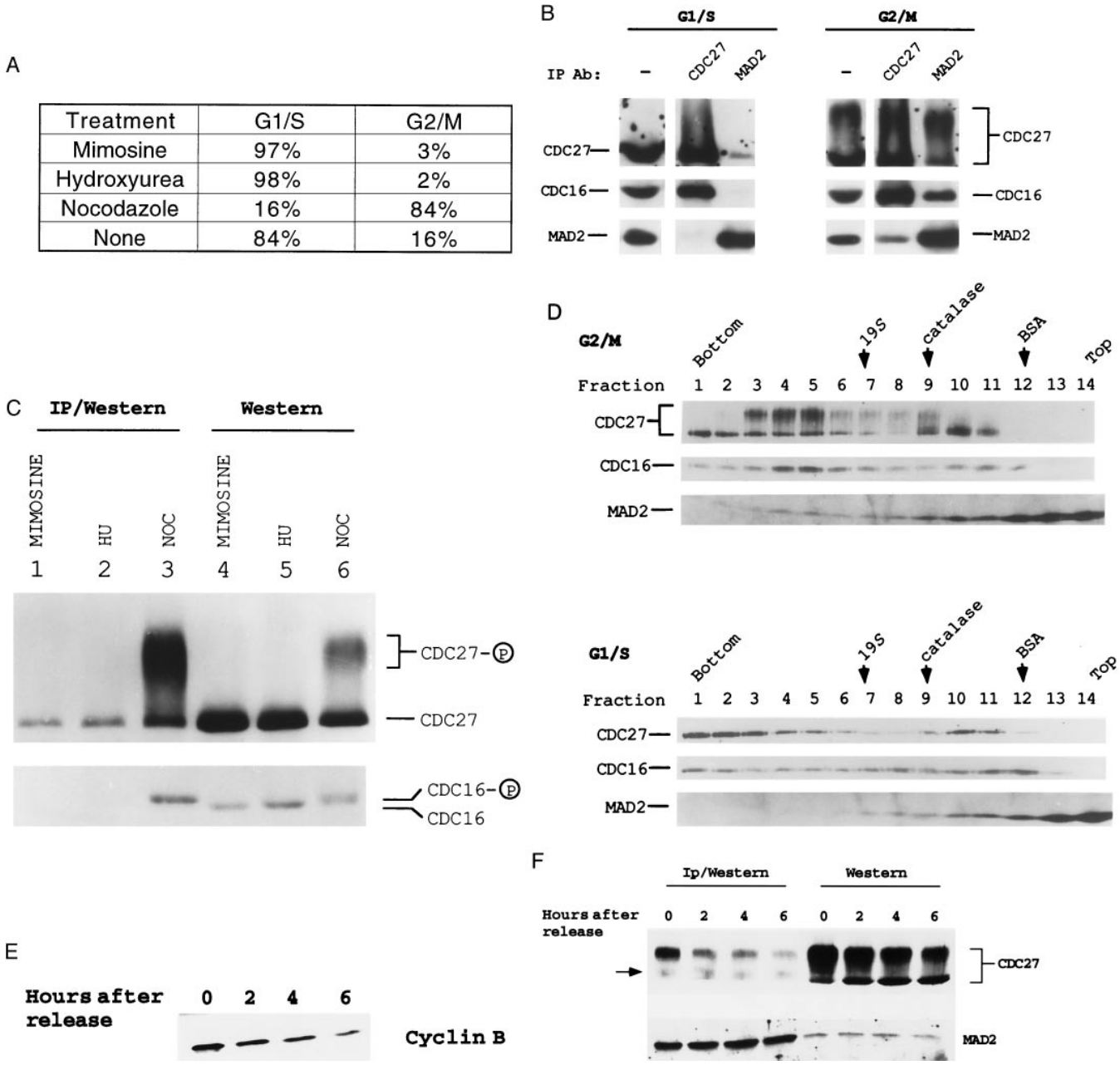

FIG. 1. MAD2 is associated with the cyclosome/APC *in vivo*. (*A*) The cell cycle profiles of HeLa cells treated with either 300 μM mimosine or 2 mM hydroxyurea (HU) for 12 hr, or with 100 nM NOC for 24 hr. HeLa cells were subjected to flow cytometry analysis as described (28). The cell cycle profile of untreated HeLa cells is also shown. (*B*) Coimmunoprecipitation of the cyclosome and MAD2 in HeLa cells. Extracts (1.5 mg) from HeLa cells arrested in G_1/S with mimosine or G_2/M with NOC were immunoprecipitated with either anti-MAD2 or anti-CDC27. The immunoprecipitates and HeLa extracts (75 μg per lane) were subjected to Western blot analysis as indicated. (*C*) MAD2 preferentially associates with the phosphorylated cyclosome in G_2/M. Extracts (1.5 mg) from HeLa cells arrested in G_1/S or G_2/M with the indicated treatments were immunoprecipitated with anti-MAD2. The immunoprecipitates (lanes 1–3) and HeLa extracts (lanes 4–6, 40 μg per lane) were subjected to low-percentage SDS/PAGE to resolve the phosphorylated CDC16 from the unphosphorylated one. Anti-CDC16 reacted with two closely migrating bands in G_2/M extracts, suggesting that a portion of CDC16 was phosphorylated (12) (lane 6, bottom row). (*D*) MAD2 and the phosphorylated cyclosome cosediment in glycerol gradients as a large complex. HeLa cells were arrested in G_1/S with mimosine and in G_2/M with NOC. Positions of the 19S regulatory complex of the 26S proteasome, catalase (232 kDa), and BSA (67 kDa) are shown. (*E*) Immunoblot analysis of the cyclin B levels after NOC release. HeLa cells were collected at the indicated time points after release from mitotic arrest. Equal amounts of extracts were then subjected to immunoblot analysis. (*F*) MAD2 dissociates from the cyclosome once the mitotic checkpoint becomes inactivated. Extracts were either directly subjected to Western blot analysis (*Right*, 60 μg per lane) or immunoprecipitated (1 mg extract) with the affinity-purified anti-MAD2 and the immunoprecipitates were then subjected to immunoblot analysis (*Left*). A background band in anti-MAD2 immunoprecipitates is indicated by an arrow. Note that anti-MAD2 antibodies primarily immunoprecipitated the phosphorylated forms of CDC27.

phase extracts. Cyclin Δ90 activates M phase promoting factor and causes a mitotic arrest (Δ90 arrest), in which the cyclin degradation machinery is activated and constitutively degrades full-length cyclin B. Addition of MAD2 did not prevent the elevation of H1 kinase activity, indicating that the extract had indeed entered mitosis (data not shown). As shown in Fig. 3 *A* and *B*, MAD2 inhibited cyclin B2 proteolysis in a dose-dependent manner. Inhibition of cyclin B ubiquitination and proteolysis was significant even at concentrations of MAD2 as low as 20 μg/ml (0.7 μM). Moreover, the effect was specific for MAD2. Preincubation of MAD2 with affinity-purified anti-MAD2 antibodies prevented stabilization of cyclin B2 (Fig. 3*C*).

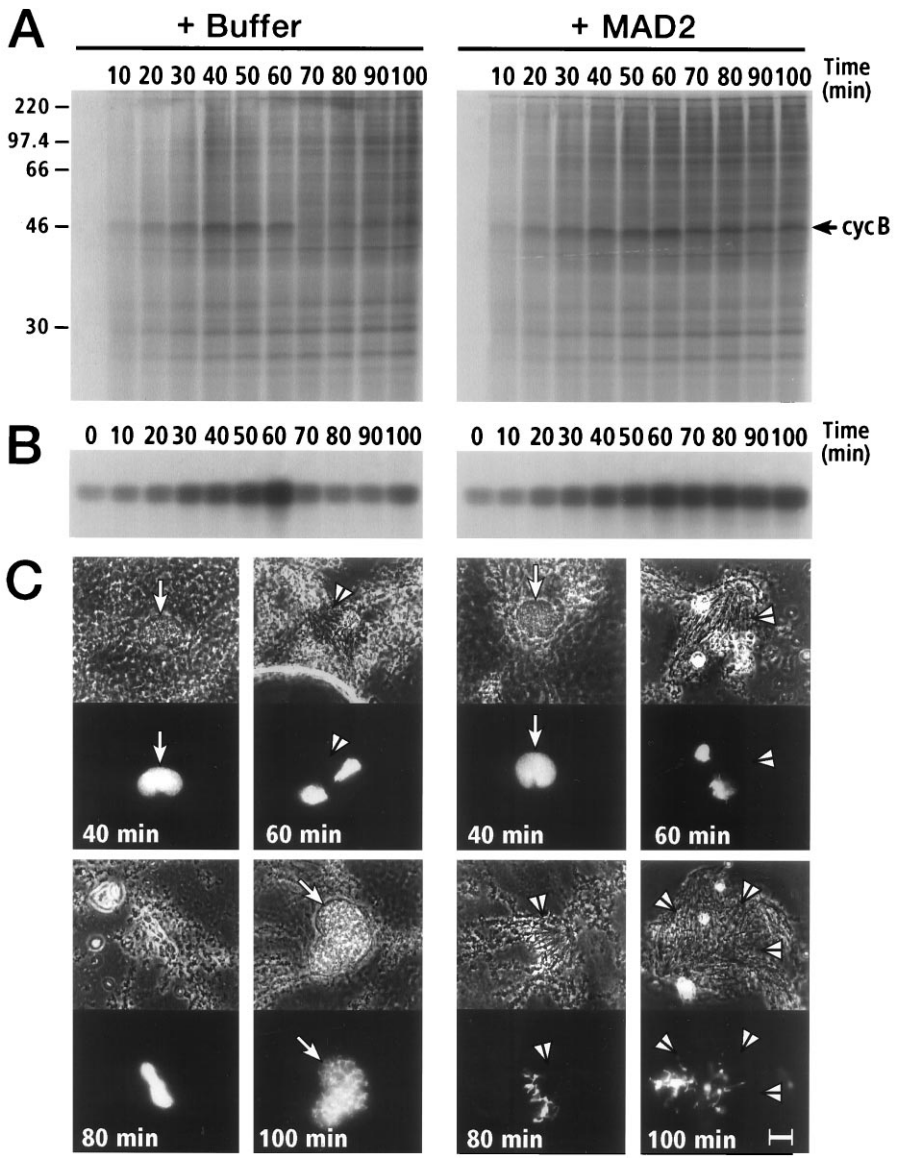

FIG. 2. Inhibition of mitotic progression of cycling *Xenopus* egg extract in the presence of human MAD2 (50 μg/ml). (*A*) Cyclin B turnover in the absence and presence of MAD2. The position of cyclin B is indicated by the arrow. (*B*) Effect of MAD2 on H1 kinase activity of cycling extracts. (*C*) Effect of MAD2 on nuclear morphology in cycling extracts. Each pair of images shows a phase contrast image (*Upper*) and an image of fluorescent Hoechst staining for DNA (*Lower*). Arrows indicate nuclear envelopes and arrowheads indicate mitotic spindles. (Bar = 10 μm.)

Δ90-arrested extracts were also produced in the absence of MAD2 to allow full activation of the cyclosome after which, MAD2 was added, and its effect on cyclin proteolysis examined. The results were consistent with the data presented in Fig. 3, except that 10-fold more MAD2 was needed to inhibit cyclin proteolysis (data not shown). This indicates that MAD2 may be more efficient at preventing the activation of the cyclosome than inhibiting a fully activated cyclosome, perhaps due to partial exclusion of the added MAD2 from the activated complexes. Nonetheless, the inhibitory effect of MAD2 on cyclin B proteolysis remained specific: neither recombinant S5b (a subunit of the 26S proteasome) nor BSA at comparable levels interfered with cyclin degradation (data not shown). Moreover, the exogenous MAD2 associated with the *Xenopus* cyclosome as shown by immunoprecipitation (Fig. 3 *D*).

To directly assay the effect of MAD2 on the cyclin Ub-ligase activity in *Xenopus* extracts, methylated Ub was employed because it causes a buildup of methylated Ub-cyclin B conjugates (26). In the presence of MAD2, cyclin B ubiquitination was substantially reduced (Fig. 4). Similar results were observed in extracts in which Δ90-arrest was induced prior to the addition of MAD2 (data not shown). Finally, cyclin ubiquitination was not inhibited in the presence of S5a, a Ub-chain binding component of the 26S proteasome that inhibits cyclin B degradation in Δ90 extracts (unpublished results, ref. 30). These data indicate that MAD2 inhibits the cyclosome /APC in *Xenopus* extracts.

To confirm that inhibition of cyclin B degradation was due to its failure to become ubiquitinated, we analyzed the effect of MAD2 on various components of the Ub-proteasome system: Ub conjugation by a series of enzymes (E1-E3), deconjugation by isopeptidases, and proteolysis of conjugated proteins by the 26S proteasome. Fig. 5*A* shows that degradation of ^{125}I-lysozyme-Ub conjugates was unaffected by MAD2. By contrast, conjugate degradation was inhibited by S5a (30). Isopeptidase activity was monitored by measuring the regeneration of ^{125}I-lysozyme from ^{125}I-lysozyme-Ub conjugates (24). As shown in Fig. 5*B*, MAD2 had no effect on isopeptidase activity. Likewise, MAD2 did not inhibit overall ^{125}I-Ub conjugation to cellular proteins (Fig. 5*C*). Thus, MAD2 appears to preferentially target the cyclin Ub-ligase activity and not other ligases of the Ub-proteasome system. Finally, MAD2

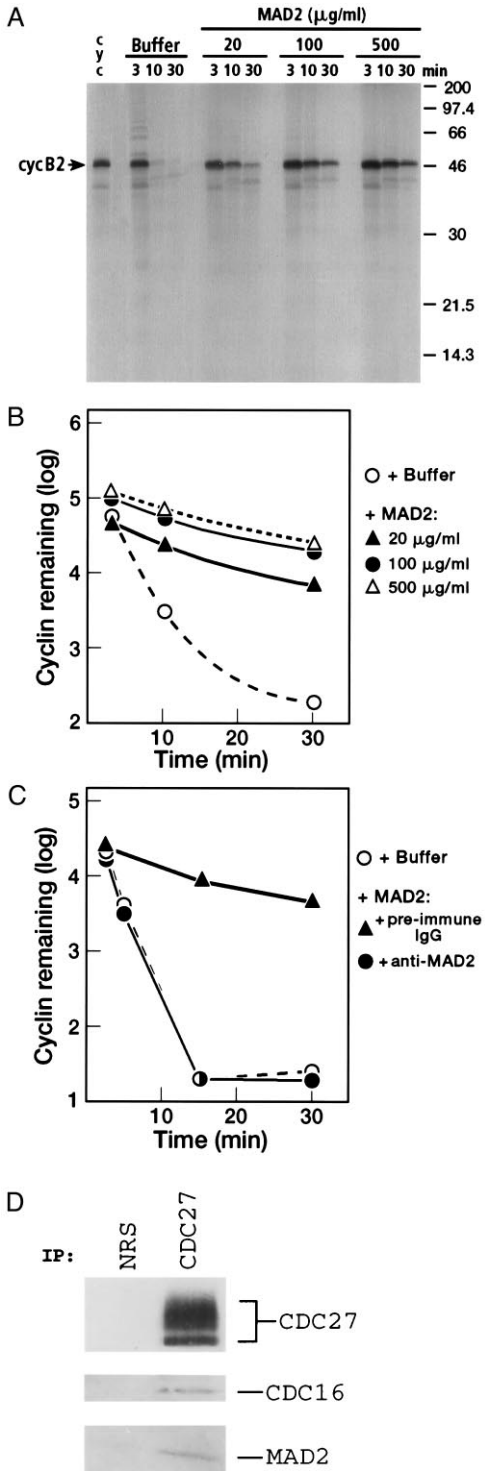

FIG. 3. Inhibition of [^{35}S]cyclin B2 proteolysis in Δ90-arrested *Xenopus* egg extracts by human MAD2. (*A*) Dose-dependent inhibition of [^{35}S]cyclin B2 degradation by MAD2 in Δ90-arrested extracts. Different concentrations of MAD2 were used in the assay as indicated, with buffer (10 mM Tris·HCl, pH 7.4/10 mM NaCl) used as a control. (*B*) Cyclin B2 degradation in the presence of different concentrations of MAD2 was quantitated by PhosphorImager analysis. The amount of [^{35}S]cyclin B2 remaining in the assay mixture *vs.* time is expressed as the logarithm of the relative density of the cyclin B band. (*C*) [^{35}S]cyclin B2 degradation in the presence of anti-MAD2 antibodies. MAD2 (3.75 μg) was preincubated with 10 μg of either preimmune IgG or affinity-purified anti-MAD2 antibodies (22) for 40 min at 23°C, and then added to Δ90-arrested extracts. (Final concentration of MAD2 in the assay was 0.25 mg/ml). The amount of [^{35}S]cyclin B2 remaining in the assay vs. time was determined as described in *B*. (*D*) Coimmunoprecipitation of exogenously added MAD2 with *Xenopus* egg cyclosome components. MAD2 (0.5 mg/ml) was added to Δ90-arrested extract and immunoprecipitated with anti-CDC27 antibodies or normal rabbit serum (NRS) as a control.

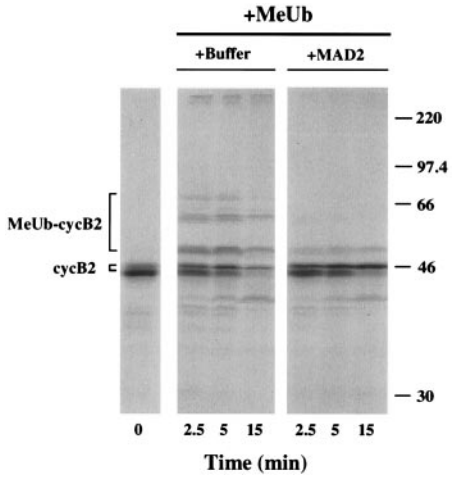

FIG. 4. Inhibition of [^{35}S]cyclin B2-methylated UB conjugation in Δ90-arrested extracts by MAD2. Cyclin Δ90 and either MAD2 (50 μg/ml) or buffer (10 mM Tris·HCl, pH 7.4/10 mM NaCl) were added to interphase extract and incubated for 40 min at 23°C. The extract (20 μl) was transferred to an Eppendorf tube containing 32 μg lyophilized methylated Ub (1.6 mg/ml final concentration) and incubated for further 10 min prior to the addition of [^{35}S]cyclin B2. The [^{35}S]cyclin degradation assay was performed as described in *Materials and Methods*. Methylated Ub was prepared as described (29).

is not a competitive substrate for the cyclosome because radiolabeled MAD2-Ub conjugates have not been detected and the levels of MAD2 in the extract remain constant throughout the incubation period (unpublished results). Taken together, our data indicate that MAD2 acts to specifically inhibit the Ub ligase activity of the cyclosome.

The *in vivo* and *in vitro* observations reported here provide a biochemical clue as to how MAD2 executes the mitotic checkpoint. The *in vivo* association data suggests that a complex including MAD2 and the cyclosome is formed during mitotic checkpoint activation and dissociates once the checkpoint is satisfied. *In vitro*, the consequence of forcing this interaction by the addition of exogenous MAD2 was to inhibit the cyclin B ubiquitination by the cyclosome and is likely to affect the ubiquitination and degradation of other noncyclin substrates involved in the metaphase-anaphase transition (31–33). Interestingly, it has been shown recently in the fission yeast *Schizosaccharomyces pombe* that MAD2 behaves genetically as a negative regulator of the cyclosome and that overexpression leads to mitotic arrest (36) in support of the model being proposed here.

The biochemical mechanism that promotes the interaction of MAD2 with the cyclosome during checkpoint activation is unknown, but may rely on the observed preferential association of MAD2 with the phosphorylated forms of the cyclosome and/or changes in MAD2 localization. The recent localization of a portion of MAD2 (21, 22) and BIME (C. Hoog, personal communication) at the kinetochore during prometaphase supports the notion that interaction of MAD2 with a small fraction of the cyclosome may be critical for MAD2 activity. We propose that this association is relieved in a coordinate manner when the checkpoint is satisfied. Whereas inhibition of cyclin B degradation by exogenously added MAD2 in *Xenopus* extracts is probably due to titration of the cyclosome, it is unclear whether MAD2 must first associate with other cellular components to effect this inhibition. Finally, whether MAD2 interacts with the cyclosome during a normal mitosis is cur-

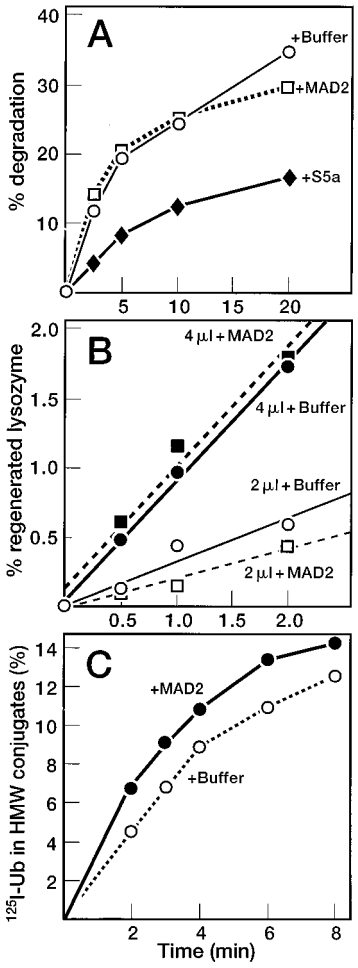

FIG. 5. Effects of MAD2 on the Ub-proteasome system in Δ90-arrested extracts. (*A*) Degradation of Ub-^{125}I-lysozyme conjugates in Δ90-arrested extract in the presence of MAD2 or subunit 5a (S5a) of the 26S proteasome. (*B*) Isopeptidase activity in Δ90-arrested extracts. Δ90 extract was incubated with either buffer (circles) or MAD2 (squares) for 10 min at 23°C. An aliquot (2 μl (○ and □) or 4 μl (● and ■) was then added to 20 μl of Ub-^{125}I-lysozyme conjugates and 0.5 μl ATP-regenerating system to assay for isopeptidase activity as described under *Materials and Methods*. (*C*) Overall Ub-conjugating activity of Δ90-arrested extracts in the absence and presence of MAD2.

rently under investigation. MAD2 could prevent premature exit from mitosis (37) or high chromosome loss rates (38), events observed under normal growth conditions in eukaryotic cells with defective mitotic checkpoints.

Although our data indicates that MAD2 functions as an effector by targeting the cyclosome, recent evidence implies that it may also function as a sensor in the checkpoint pathway. Since a portion of MAD2 is localized at the kinetochore prior to the metaphase-anaphase transition in HeLa cells (21, 22), it could act locally to monitor kinetochore attachment to the spindle and to prevent the cyclosome from ubiquitinating the putative inhibitor(s) of sister chromatid segregation. Consistent with these ideas, it has been shown that *MAD2* functions both upstream and downstream of *MAD1* in budding yeast to arrest cells in mitosis (34, 35). The experiments presented here indicate that inhibition of the cyclosome by MAD2 is a component of the downstream signaling pathway. Discovering how MAD2 interacts with other cellular components will be essential for complete understanding of the mechanism underlying mitotic checkpoint function. Nonetheless, our results provide a biochemical explanation as to how the mitotic checkpoint maintains high levels of cyclin B and keeps sister chromatids from segregating.

We thank Tim Hunt for the *Xenopus* cyclin B2 clone, Michael Glotzer for the *Arbacia* cyclin Δ90 clone, Philip Hieter for the anti-CDC16 and anti-CDC27 antibodies, and Christer Hoog for communicating unpublished results. Y.L. is a Jack and Susan Rudin Scholar in Biomedical Sciences. The studies were supported by grants from the National Institutes of Health (M.R. and R.B.), The Lucille P. Markey Charitable Trust (M.R.), the National Science Foundation, and the National Cancer Institute (R.B.).

1. Deshaies, R. J. (1995) *Trends Cell Biol.* **5,** 428–434.
2. King, R. W., Deshaies, R. J., Peters, J.-M. & Kirschner, M. W. (1996) *Science* **274,** 1652–1659.
3. Hershko, A. & Ciechanover, A. (1992) *Annu. Rev. Biochem.* **61,** 761–807.
4. Rechsteiner, M., Hoffman, L. & Dubiel, W. (1993) *J. Biol. Chem.* **268,** 6065–6068.
5. Irniger, S., Piatti, S., Michaelis, C. & Nasmyth, K. (1995) *Cell* **81,** 269–278.
6. Amon, A., Irniger, S. & Nasmyth, K. (1994) *Cell* **77,** 1037–1050.
7. Brandeis, M. & Hunt, T. (1996) *EMBO J.* **15,** 5280–5289.
8. Sudakin, V., Ganoth, D., Dahan, A., Heller, H., Hershko, J., Luca, F. C., Ruderman, J. V & Hershko, A. (1995) *Mol. Biol. Cell* **6,** 185–198.
9. King, R. W., Peters, J.-M., Tugendreich, S., Rolfe, M., Hieter, P. & Kirschner, M. W. (1995) *Cell* **81,** 279–288.
10. Zachariae, W. & Nasmyth, K. (1996) *Mol. Biol. Cell* **7,** 791–801.
11. Zachariae, W., Shin, T. H., Galova, M., Obermaier, B. & Nasmyth, K. (1996) *Science* **274,** 1201–1204.
12. Peters, J.-M., King, R. W., Hoog, C. & Kirschner, M. W. (1996) *Science* **274,** 1199–1201.
13. Lahav-Baratz, S., Sudakin, V., Ruderman, J. V. & Hershko, A. (1995) *Proc. Natl. Acad. Sci. USA* **92,** 9303–9307.
14. Tugendreich, S., Tomkiel, J., Earnshaw, W. & Hieter, P. (1995) *Cell* **81,** 261–268.
15. Lamb, J. R., Michaud, W. A., Sikorski, R. S. & Hieter, P. A. (1994) *EMBO J.* **13,** 4321–4328.
16. Osmani, S. A., Engle, D. B., Doonan, J. H. & Morris, N. R. (1988) *Cell* **52,** 241–251.
17. Holloway, S. L., Glotzer, M., King, R. W. & Murray, A. W. (1993) *Cell* **73,** 1393–1402.
18. Hartwell, L. H. & Kastan, M. B. (1994) *Science* **266,** 1821–1828.
19. Murray, A. W. (1996) *Curr. Opin. Genet. Dev.* **5,** 5–11.
20. Elledge, S. J. (1996) *Science* **274,** 1664–1672.
21. Chen, R.-H., Waters, J. C., Salmon, E. D. & Murray, A. W. (1996) *Science* **274,** 242–246.
22. Li, Y. & Benezra, R. (1996) *Science* **274,** 246–248.
23. Murray, A. W. & Kirschner, M. W. (1989) *Nature (London)* **339,** 275–280.
24. Mahaffey, D. T., Yoo, Y. & Rechsteiner, M. (1993) *J. Biol. Chem.* **268,** 21205–21211.
25. Glotzer, M., Murray, A. W. & Kirschner, M. W. (1991) *Nature (London)* **349,** 132–138.
26. Mahaffey, D. T., Yoo, Y. & Rechsteiner, M. (1995) *FEBS Lett.* **370,** 109–112.
27. Hough, R. & Rechsteiner, M. (1986) *J. Biol. Chem.* **261,** 2391–2399.
28. Firpo, E. J., Hoff, A., Solomon, M. J. & Roberts, J. M. (1994) *Mol. Cell. Biol.* **14,** 4889–4901.
29. Hershko, A. & Heller, H. (1985) *Biochem. Biophys. Res. Commun.* **128,** 1079–1086.
30. Deveraux, Q., van Nocker, S., Mahaffey, D., Vierstra, R. & Rechsteiner, M. (1995) *J. Biol. Chem.* **270,** 29660–29663.
31. Yamamoto A., Guacci, V. & Koshland, D. (1996) *J. Cell Biol.* **133,** 85–97.
32. Cohen-Fix, O., Peters, J.-M., Kirschner, M. W. & Koshland, D. (1996) *Genes Dev.* **10,** 3081–3093.
33. Funabiki, H., Yamano, H., Kumada, K., Nagao, K., Hunt, T. & Yanagida, M. (1996) *Nature (London)* **381,** 438–441.
34. Hardwick, K. & Murray, A. W. (1995) *J. Cell Biol.* **131,** 709–720.
35. Hardwick, K. G., Weiss, E., Luca, F. C., Winey, M. & Murray, A. W. (1996) *Science* **273,** 953–956.
36. He, X., Patterson, T. E. & Sazer, S. (1997) *Proc. Natl. Acad. Sci. USA* **94,** 7965–7970.
37. Taylor, S. S. & McKeon, F. (1997) *Cell* **89,** 727–735.
38. Li, R. & Murray, A. W. (1991) *Cell* **66,** 519–531.